Light-shining-through-wall cavity setups for probing ALPs

Dmitry Salnikov[1,2]
salnikov.dv16@physics.msu.ru
in collaboration with
Maxim Fitkevich[1,3], Dmitry Kirpichnikov[1] and Petr Satunin[1]

[1]Institute for Nuclear Research of the Russian Academy of Science
[2]Lomonosov Moscow State University
[3]Moscow Institute of Physics and Technology

JETP Letters **117** (2023) [arXiv:2303.15996]

The research was supported by the RSF grant №21-72-10151.

October 06, 2023

Introduction

- Axions and axion-like particles (ALPs) are hypothetical pseudo-scalar particles. They are massive and electrically neutral.
- Axion as CP-strong problem solution [Peccei-Quinn, 1977].
- Axions and ALPs as a part of dark matter content [Preskill, Abbott, Dine, 1982].
- Interaction with EM-field is described by the following term of the Lagrangian and the corresponding vertex:

$$\mathcal{L}_{\text{int}} = -\frac{g_{a\gamma\gamma}}{4}\, a\, F_{\mu\nu}\tilde{F}^{\mu\nu}$$

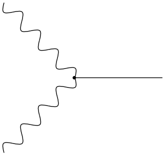

The mass of m_a and the coupling constant of $g_{a\gamma\gamma}$ are related for QCD axion as follows, $g_{a\gamma\gamma} = 10^{-10}\,\text{GeV}^{-1}\left(\frac{m_a}{1\,\text{eV}}\right)$. These parameters are independent for ALPs.

Detection methods

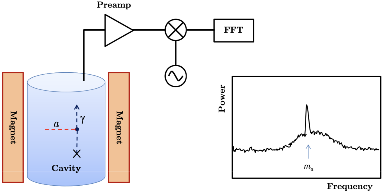

a)

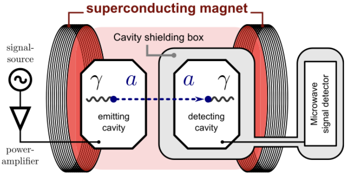

b)

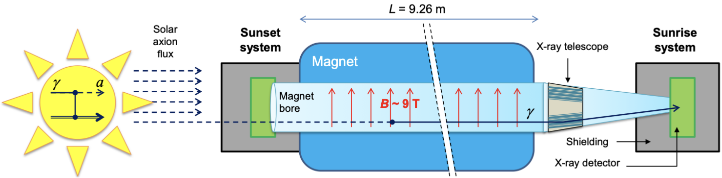

c)

Figure 1 – The experiments for axions and ALPs search.
a) haloscope, b) LSW, c) helioscope (CAST).

Current limitations

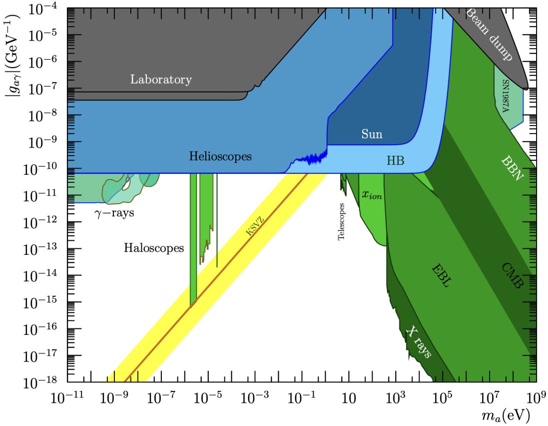

Figure 2 – The current limitations on parameters $(m_a, g_{a\gamma\gamma})$ for QCD axions and ALPs.

LSW experimental setups

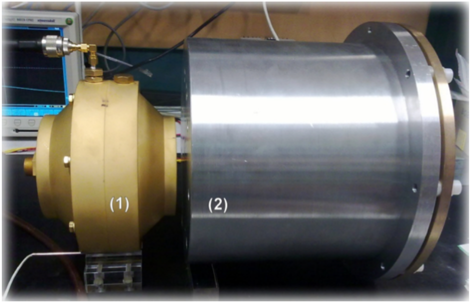

FIG. 7: Photo of emitting cavity (1) and shielding enclosure (2) containing the identical detecting cavity. For ALP search, both parts were placed in the bore of a solenoid magnet with the same arrangement as shown in the picture.

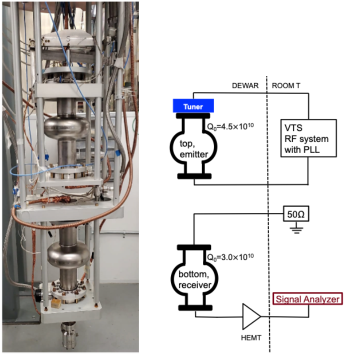

FIG. 1. Left: The experimental setup for the Dark SRF experiment consisting of two 1.3 GHz cavities. Right: A sketch of the Dark SRF electronic system.

Figure 3 – The experimental setups photos. The left panel presents the CROWS experiment at CERN [Betz *et al.*, 2013]. The right panel presents the current Fermilab experimental setup [Romanenko *et al.*, 2023]. Results were published for Dark photons search only. The SRF experimental setup at CERN is projecting [Bogorad *et al.*, 2023].

Motivation and aims

- The LSW cavity setups are being developed at the moment
- The problem of their sensitivity improvement is important
- The research aims were
  - comparison of various cavity types (normal conducting and superconducting RF) schemes of the LSW cavity setups
  - finding the optimal geometrical configuration
  - discussion of schemes technical features

Experimental model scheme

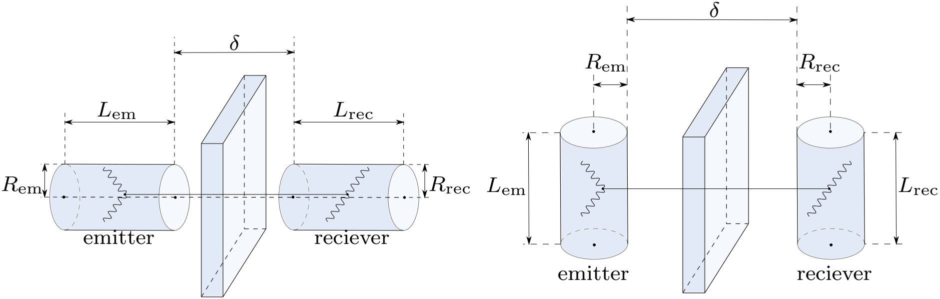

Figure 4 – The experimental model schemes for two cavity orientations: coaxial (the left panel) and parallel (the right panel).

Cavity type	B_0	B_{ext}	Q	P
Normal conducting RF	0.01 T	3 T	10^5	100 kW
Superconducting RF	0.1 T	-	10^{10}	0.1 kW

Table 1 – The basic characteristics of normally conducting RF and SRF cavities. Four setups were considered:
i) RF+RF, ii) SRF+SRF, iii) SRF+RF, iv) RF+SRF.

Theory

- The motion equations

$$(\partial_\mu \partial^\mu + m_a^2)\, a = -\frac{g_{a\gamma\gamma}}{4} F_{\mu\nu} \tilde{F}^{\mu\nu}, \tag{1}$$

$$\partial_\mu F^{\mu\nu} = -g_{a\gamma\gamma}\, \tilde{F}^{\mu\nu} \partial_\mu a = j_a^\nu . \tag{2}$$

- In the electric and magnetic field terms it reads

$$(\partial_\mu \partial^\mu + m_a^2)\, a = g_{a\gamma\gamma}\, (\vec{E} \cdot \vec{B})\ , \tag{3}$$

$$(\vec{\nabla} \cdot \vec{E}) = \rho_a, \quad [\vec{\nabla} \times \vec{B}] = \frac{\partial \vec{E}}{\partial t} + \vec{j}_a, \tag{4}$$

where

$$\rho_a = -g_{a\gamma\gamma}(\vec{\nabla} a \cdot \vec{B})\ , \quad \vec{j}_a = g_{a\gamma\gamma}([\vec{\nabla} a \times \vec{E}] + \dot{a}\vec{B})\ . \tag{5}$$

Generated signal

- The exact Klein-Gordon equation solution is

$$a(t,\vec{x})=g_{a\gamma\gamma}E_0^{\rm em}B_0^{\rm em}{\rm Re}\left[\int\limits_{V_{\rm em}} d^3x'\,(\vec{\mathcal{E}}\cdot\vec{\mathcal{B}})(\vec{x}')\,\frac{e^{ik_a|\vec{x}-\vec{x}'|-i\omega_a t}}{4\pi|\vec{x}-\vec{x}'|}\right]. \qquad (6)$$

- The exact Maxwell's equations solution is

$$\vec{E}(t,\vec{x})\simeq{\rm Re}[G\vec{\mathcal{E}}_s(\vec{x})e^{-i\omega_s t}],\quad \vec{B}(t,\vec{x})\simeq{\rm Re}[G\vec{\mathcal{B}}_s(\vec{x})e^{-i\omega_s t}], \qquad (7)$$

$$G=-\frac{Q_{\rm rec}}{\omega_s}\cdot\frac{1}{V_{\rm rec}}\int\limits_{V_{\rm rec}} d^3x\,(\vec{\mathcal{E}}_s^*\cdot\vec{j}_a)=iQ_{\rm rec}g_{a\gamma\gamma}^2E_0^{\rm em}B_0^{\rm em}B_0^{\rm rec}V_{\rm em}V_{\rm rec}\mathcal{G}\delta^{-1}, \quad (8)$$

$$\mathcal{G}=\int\limits_{V_{\rm rec}}\frac{d^3x}{V_{\rm rec}}\int\limits_{V_{\rm em}}\frac{d^3x'}{V_{\rm em}}\,(\vec{\mathcal{E}}\cdot\vec{\mathcal{B}})^*(\vec{x})\,(\vec{\mathcal{E}}\cdot\vec{\mathcal{B}})(\vec{x}')\,\frac{e^{ik_a|\vec{x}-\vec{x}'|}}{4\pi}\,\frac{\delta}{|\vec{x}-\vec{x}'|}. \qquad (9)$$

- For both cases of $\omega_a=\omega_0$ and $\omega_a=\omega_1+\omega_2$ EM-invariant reads

$$(\vec{\mathcal{E}}\cdot\vec{\mathcal{B}})=(\vec{\mathcal{E}}_0\cdot\vec{\mathcal{B}}_{\rm ext}),\quad (\vec{\mathcal{E}}\cdot\vec{\mathcal{B}})_+=\frac{1}{2}(\vec{\mathcal{E}}_1\cdot\vec{\mathcal{B}}_2+\vec{\mathcal{E}}_2\cdot\vec{\mathcal{B}}_1). \qquad (10)$$

Experiment sensitivity

- The signal power

$$P_{\text{signal}} = \frac{\omega_s}{Q_{\text{rec}}} \int\limits_{V_{\text{rec}}} d^3x \, \langle |\vec{E}^2(\vec{x},t)| \rangle_t = \frac{\omega_s}{Q_{\text{rec}}} \cdot \frac{1}{2} |G|^2 V_{\text{rec}} \,, \qquad (11)$$

- The radiometric equation

$$\text{SNR} = \frac{P_{\text{signal}}}{P_{\text{noise}}} \cdot \sqrt{t \Delta\nu} \,, \qquad (12)$$

where $P_{\text{noise}} = T\Delta\nu$ – the thermal noise power ($\omega_s \ll T$).

- The sensitivity estimation

$$g_{a\gamma\gamma} = \left[\frac{2\delta^2 T \, \text{SNR}}{\omega_s Q_{\text{rec}} E^2_{0,\text{em}} B^2_{0,\text{em}} B^2_{0,\text{rec}} V^2_{\text{em}} V_{\text{rec}} |\mathcal{G}|^2} \right]^{\frac{1}{4}} \left(\frac{\Delta\nu}{t} \right)^{\frac{1}{8}} \,, \qquad (13)$$

where $\Delta\nu = \dfrac{\nu_s}{Q_{\text{rec}}}$ or $\Delta\nu = \dfrac{1}{t}$ [Bogorad, 2019]

RF + RF scheme sensitivity

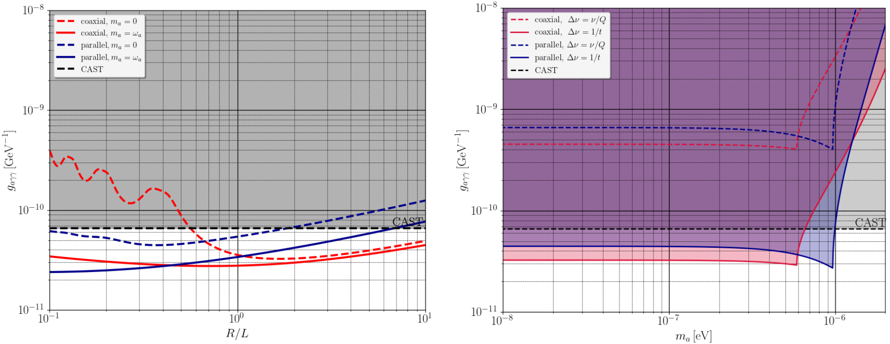

Figure 5 – The sensitivity dependence $g_{a\gamma\gamma}$ for the RF+RF scheme on the R/L ratio for the cases of $m_a = \omega_a$ and $m_a = 0$ (the left panel) and on the mass in the case of an optimal value of the R/L ratio (the right panel). The coaxial and parallel orientations are considered. The cavities volume is $V = 1\,\text{m}^3$, the distance between cavities walls $\delta = 0.5$ m, the EM-mode is TM_{010}, the experiment duration is $t = 10^6$ s.

SRF + SRF scheme sensitivity

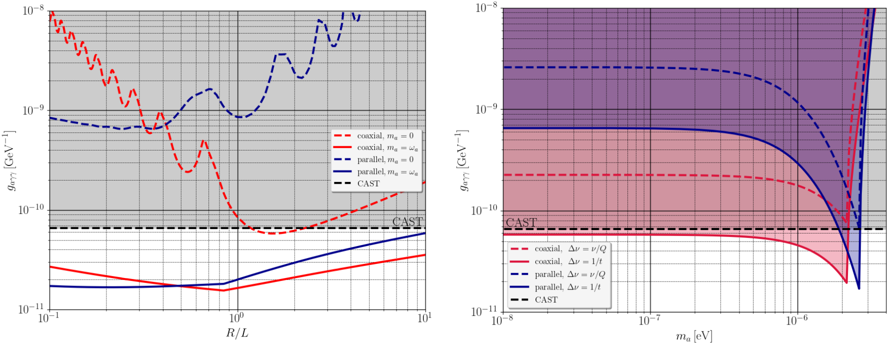

Figure 6 – The sensitivity dependence $g_{a\gamma\gamma}$ for the SRF+SRF scheme on the R/L ratio for the cases of $m_a = \omega_a$ and $m_a = 0$ (the left panel) and on the mass in the case of an optimal value of the R/L ratio (the right panel). The coaxial and parallel orientations are considered. The cavities volume is $V = 1\,\mathrm{m}^3$, the distance between cavities walls $\delta = 0.5$ m, the EM-modes are $\mathrm{TM}_{010}+\mathrm{TE}_{011}$, the experiment duration is $t = 10^6$ s.

SRF + RF scheme sensitivity

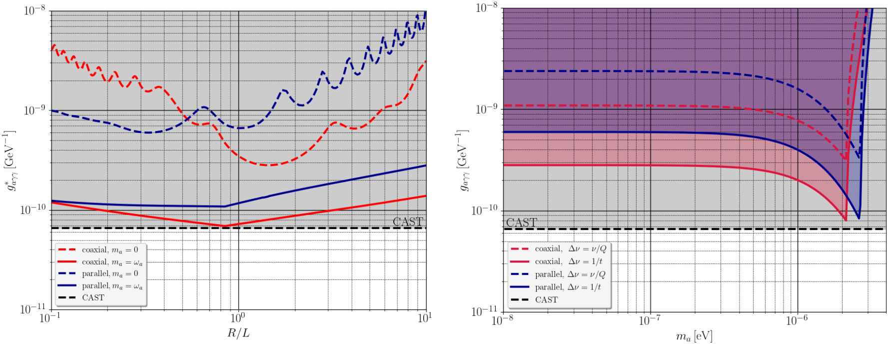

Figure 7 – The sensitivity dependence $g_{a\gamma\gamma}$ for the SRF+RF scheme on the R/L ratio for the cases of $m_a = \omega_a$ and $m_a = 0$ (the left panel) and on the mass in the case of an optimal value of the R/L ratio (the right panel). The coaxial and parallel orientations are considered. The emitter volume is $V = 1\,\mathrm{m}^3$, the distance between cavities walls $\delta = 0.5$ m, the emitter pump EM-modes are $\mathrm{TM}_{010}+\mathrm{TE}_{011}$, the signal receiver mode is TM_{010}, the experiment duration is $t = 10^6$ s.

RF + SRF scheme sensitivity

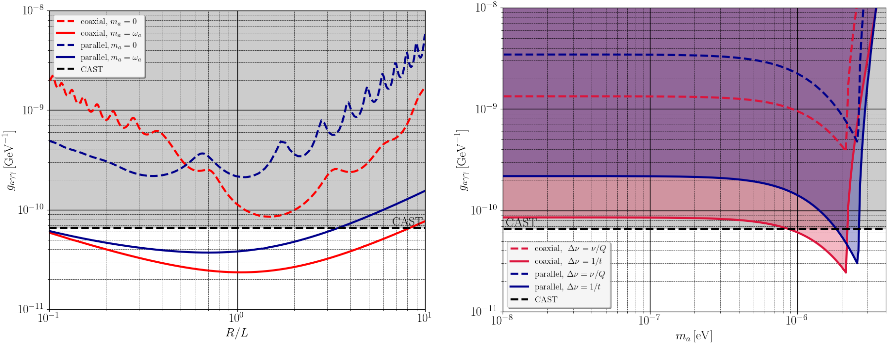

Figure 8 – The sensitivity dependence $g_{a\gamma\gamma}$ for the RF+SRF scheme on the R/L ratio for the cases of $m_a = \omega_a$ and $m_a = 0$ (the left panel) and on the mass in the case of an optimal value of the R/L ratio (the right panel). The coaxial and parallel orientations are considered. The receiver volume is $V = 1\,\mathrm{m}^3$, the distance between cavities walls $\delta = 0.5$ m, the pump emitter EM-mode is TM_{010}, the receiver modes are $\mathrm{TM}_{010}+\mathrm{TE}_{011}$, the experiment duration is $t = 10^6$ s.

Results and conclustions

Scheme type	$B_0^{\mathrm{em},(1)}$	$B_0^{\mathrm{em},(2)}$	B_0^{rec}	Q_{rec}	P_{em}	$\lvert\mathcal{G}\rvert$	$g_{a\gamma\gamma}$
RF em. + RF rec.	$0.01\,\mathrm{T}$	$3\,\mathrm{T}$	$3\,\mathrm{T}$	10^5	$100\,\mathrm{kW}$	10^{-2}	$3\times10^{-11}\,\mathrm{GeV}^{-1}$
SRF em. + SRF rec.	$0.1\,\mathrm{T}$	$0.1\,\mathrm{T}$	$0.1\,\mathrm{T}$	10^{10}	$0.1\,\mathrm{kW}$	10^{-3}	$5\times10^{-11}\,\mathrm{GeV}^{-1}$
SRF em. + RF rec.	$0.1\,\mathrm{T}$	$0.1\,\mathrm{T}$	$3\,\mathrm{T}$	10^5	$0.1\,\mathrm{kW}$	10^{-3}	$3\times10^{-10}\,\mathrm{GeV}^{-1}$
RF em. + SRF rec.	$0.01\,\mathrm{T}$	$3\,\mathrm{T}$	$0.1\,\mathrm{T}$	10^{10}	$100\,\mathrm{kW}$	10^{-3}	$9\times10^{-11}\,\mathrm{GeV}^{-1}$

Table 2 – The comparison of various schemes characteristics values. The geometric form-factor $|\mathcal{G}|$ and the experiment sensitivity $g_{a\gamma\gamma}$ are presented for the optimal R/L ratio for coaxial orientation and the low masses limit (area of $m_a \lesssim \omega_a/2$).

- Both RF+RF and SRF+SRF schemes allow to obtain similar values of the sensitivity at the level of $g_{a\gamma\gamma} \simeq (3-5)\times 10^{-11}\mathrm{GeV}^{-1}$. Mixed schemes expectations are several orders weaker.
- The coaxial orientation with the ratio of $R/L \simeq 1.6$ is the most optimal geometrical configuration.
- The narrowest bandwidth of $\Delta\nu = 1/t$ is the important issue.
- The disadvantage of RF+RF scheme is high emitter power, the disadvantage of SRF+SRF scheme is a more complicated signal photons detection against the pump mode background.

Thank you!

arXiv:2303.15996

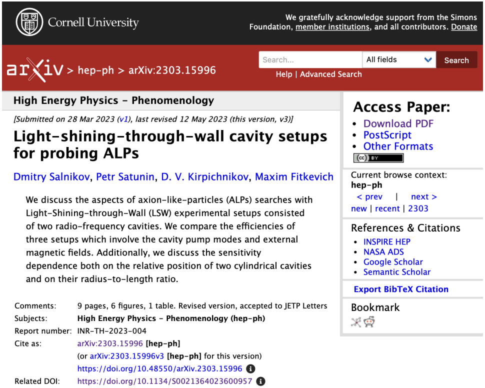

Cornell University

We gratefully acknowledge support from the Simons Foundation, member institutions, and all contributors. Donate

arXiv > hep-ph > arXiv:2303.15996

Search... | All fields | Search

Help | Advanced Search

High Energy Physics – Phenomenology

[Submitted on 28 Mar 2023 (v1), last revised 12 May 2023 (this version, v3)]

Light-shining-through-wall cavity setups for probing ALPs

Dmitry Salnikov, Petr Satunin, D. V. Kirpichnikov, Maxim Fitkevich

We discuss the aspects of axion-like-particles (ALPs) searches with Light-Shining-through-Wall (LSW) experimental setups consisted of two radio-frequency cavities. We compare the efficiencies of three setups which involve the cavity pump modes and external magnetic fields. Additionally, we discuss the sensitivity dependence both on the relative position of two cylindrical cavities and on their radius-to-length ratio.

Comments:	9 pages, 6 figures, 1 table. Revised version, accepted to JETP Letters
Subjects:	**High Energy Physics – Phenomenology (hep-ph)**
Report number:	INR-TH-2023-004
Cite as:	arXiv:2303.15996 **[hep-ph]**
	(or arXiv:2303.15996v3 **[hep-ph]** for this version)
	https://doi.org/10.48550/arXiv.2303.15996
Related DOI:	https://doi.org/10.1134/S0021364023600957

Access Paper:
- Download PDF
- PostScript
- Other Formats

Current browse context:
hep-ph
< prev | next >
new | recent | 2303

References & Citations
- INSPIRE HEP
- NASA ADS
- Google Scholar
- Semantic Scholar

Export BibTeX Citation

Bookmark